Mon. Not. R. Astron. Soc. **000**, 000–000 (0000) Printed 10 September 1999 (MN LaTeX style file v1.3)

Two measures of the shape of the Milky Way's dark halo

Rob P. Olling[1⋆], Michael R. Merrifield[2†]
[1]Department of Physics and Astronomy, Rutgers University, PO Box 849, Piscataway, NJ 08855, USA
[2] School of Physics and Astronomy, University of Nottingham, University Park, Nottingham, NG7 2RD

10 September 1999

ABSTRACT

In order to test the reliability of determinations of the shapes of galaxies' dark matter halos, we have made such measurements for the Milky Way by two independent methods. First, we have combined the measurements of the over-all mass distribution of the Milky Way and the measurements of the amount of dark matter in the solar neighborhood obtained from stellar kinematics to determine the flattening of the dark halo. Second, we have used the established technique based on the variation in thickness of the Milky Way's HI layer with radius: by assuming that the HI gas is in hydrostatic equilibrium in the gravitational potential of a galaxy, one can use the observe flaring of the gas layer to determine the shape of the dark halo.

These techniques are found to produce a consistent estimate for the flattening of the dark matter halo, with a shortest-to-longest axis ratio of $q \sim 0.8$, but only if one adopts somewhat non-standard values for the distance to the Galactic centre, R_0, and the local Galactic rotation speed, Θ_0. For consistency, one requires values of $R_0 \lesssim 7.6\,\mathrm{kpc}$ and $\Theta_0 \lesssim 190\,\mathrm{km\,s^{-1}}$. The results depend on the Galactic constants because the adopted values affect both distance measurements within the Milky Way and the shape of the rotation curve, which, in turn, alter the inferred halo shape. Although differing significantly from the current IAU-sanctioned values, these upper limits are consistent with all existing observational constraints.

If future measurements confirm these lower values for the Galactic constants, then the validity of the gas layer flaring method will be confirmed. Further, dark matter candidates such as cold molecular gas and massive decaying neutrinos, which predict very flat dark halos with $q \lesssim 0.2$, will be ruled out. Conversely, if the Galactic constants were found to be close to the more conventional values, then there would have to be some systematic error in the methods for measuring dark halo shapes, so the techniques would need to include more sophisticated modelling.

Key words: Galaxy: structure - Galaxy: kinematics and dynamics - Galaxy: solar neighbourhood - Galaxy: fundamental parameters - Galaxy: stellar content - ISM: general

1 INTRODUCTION

The speed at which spiral galaxies rotate remains relatively constant out to large radii (e.g., Rubin, Ford & Thonnard 1980; Bosma 1981), which implies that they contain large amounts of dark matter. The nature of this material remains obscure, but one key diagnostic is provided by the shape of the dark matter halo, as quantified by its shortest-to-longest axis ratio, $q = c/a$. The roundest halos with $q \sim 0.8$ are predicted by galaxy formation models in which hot dark matter is dominant (Peebles 1993). Cosmological cold dark matter simulations typically result in triaxial dark halos (Warren et al. 1992) while the inclusion of gas dynamics in the simulations results in somewhat flattened, oblate, halos (Katz & Gunn 1991; Udry & Martinet 1994; Dubinski 1994) with $q = 0.5 \pm 0.15$ (Dubinski 1994). Other dark matter candidates such as cold molecular gas and massive decaying neutrinos would produce halos as flat as $q \sim 0.2$ (Pfenniger, Combes & Martinet 1994; Sciama 1990). Clearly, the determination of q for real galaxies offers a valuable test for discriminating between these cosmological models.

In Fig. 1, we summarize the existing estimates of halo shape, derived using a variety of techniques. It is evident from this figure that there is only a very limited amount of

⋆ E-mail: olling@astro.rutgers.edu
† E-mail: Michael.Merrifield@Nottingham.ac.uk

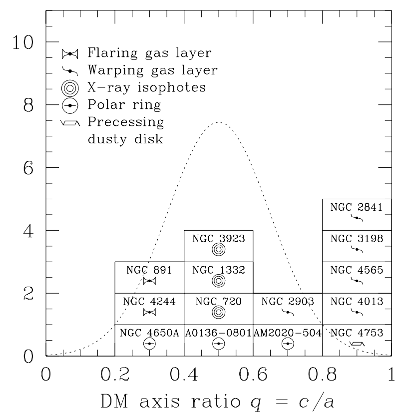

Figure 1. A summary of the existing estimates of galaxies' dark matter halo shapes as parameterized by their shortest-to-longest axis ratio, q. For each individual galaxy we indicate the identification and technique used to determine the halo's flattening: 1) Flaring gas layer (Olling 1996b; Becquaert, Combes & Viallefond 1997); 2) Warping gas layer (Hofner & Sparke 1994); 3) X-ray isophotes, (Buote & Canizares 1998); 4) Polar ring galaxies (Arnaboldi et al. 1993; Sackett et al. 1994; Sackett & Pogge 1995); 5) precessing dusty disk (Steiman-Cameron, Kormendy & Durisen 1992). The dotted line shows the predicted distribution for the shapes of halos in a cold dark matter cosmology ($q = 0.5 \pm 0.15$; Dubinski 1994).

data available for measuring the distribution of q in galaxies. Rather more worrying, though, is the fact that different techniques seem to yield systematically different answers. The warping gas layer method, in which the shape of the halo is inferred by treating any warp in a galaxy's gas layer as a bending mode in a flattened potential (Hofner & Sparke 1994), seems to imply that dark halos are close to spherical, with $q \gtrsim 0.8$. Conversely, the flaring gas layer technique, which determines the halo shape by assuming that the gas layer is in hydrostatic equilibrium in the galaxy's gravitational potential and uses the thickness of the layer as a diagnostic for the distribution of mass in the galaxy (Olling 1996b), yields much flatter halo shape estimates with $q \lesssim 0.4$. Although the numbers involved are rather small, there do seem to be real differences between the results obtained by the different methods. Thus, either these techniques are being applied to systematically different classes of galaxy, or at least some of the methods are returning erroneous results.

In order to determine which techniques are credible, we really need to apply several methods to a single galaxy, to see which produce consistent answers. As a first step towards such cross-calibration, this paper compares the shape of our own galaxy's dark matter halo as inferred by two distinct techniques:

(i) *Stellar kinematics.* Our position within the Milky Way means that we have access to information for this galaxy that cannot be obtained from other systems. In particular, it is possible to measure the total column density of material near the Sun using stellar kinematics. After subtracting off the other components, we can hence infer the local column density of dark matter. We can obtain a direct measure of the halo shape by comparing the measured value of the local column density to estimates derived from the over-all Galactic mass distribution (as derived from the rotation curve). By comparing this density in the plane of the Galaxy to the over-all mass as derived from its rate of rotation, we can obtain a direct measure of the shape of the halo.

(ii) *The flaring gas layer method.* As outlined above, this technique assumes that the HI emission in the Milky Way comes from gas in hydrostatic equilibrium in the Galactic potential, from which the shape of the dark halo is inferred. Since the results of previous applications of this method give results somewhat out of line with the other techniques, it is important to assess the method's credibility.

As well as providing a check on the validity of the flaring gas layer method, the analyses presented in this paper will also provide another useful datum on the rather sparsely populated Fig. 1.

The remainder of the paper is laid out as follows. Both of the above methods rely on knowledge of the Milky Way's rotation velocity as a function of Galactic radius – its "rotation curve" – so Section 2 summarizes the data available for estimating this quantity, and the dependence of the inferred rotation curve on the assumed distance to the Galactic centre and local rotation velocity. The analysis of the shape of the dark halo requires that we decompose the Milky Way into its visible and dark matter components, so Section 3 discusses the construction of a set of models consistent with both the photometric properties of the Galaxy, and its mass properties as inferred from the rotation curve. In Section 4 we show how these mass models can be combined with the local stellar kinematic measurements to determine the shape of the dark halo. Section 5 presents the application of the gas layer flaring technique to the mass models. Section 6 combines the results derived by the two techniques and assesses their consistency. The broader conclusions of this work are drawn in Section 7.

2 THE OBSERVED ROTATION CURVE

Our position within the Milky Way complicates the geometry when studying its structure and kinematics. It is therefore significantly harder to determine our own galaxy's rotation curve, $\Theta(R)$, than it is to derive those for external systems. More directly accessible to observation than $\Theta(R)$ is the related quantity

$$W(R) = R_0 \left[\frac{\Theta(R)}{R} - \frac{\Theta_0}{R_0} \right], \tag{1}$$

where R_0 and Θ_0 are the distance to the Galactic centre and the local circular speed. If one assumes that material in the galaxy is in purely circular motion, then some simple geometry shows that for an object at Galactic coordinates $\{l, b\}$ with a line-of-sight velocity $v_{\rm los}$, W is given by:

$$W = \frac{v_{\rm los}}{\sin l \cos b} \tag{2}$$

(Binney & Merrifield 1998). Thus, if one measures the line-of-sight velocities for a series of objects at some radius R

in the Galaxy, one has an estimate for $W(R)$. By adopting values for R_0 and Θ_0, one can then use equation (1) to determine the rotation speed at that radius.

In practice, the difficulty lies in knowing the Galactic radii of the objects one is looking at. One solution is to look at standard candles, whose distances can be estimated, and hence whose radii in the Galaxy can be geometrically derived. Alternatively, one can select the subset of some tracer – usually H I or H_2 gas – whose line-of-sight velocities and Galactic coordinates places it at the same value of W, and hence at the same radius. One can then use the properties of this cylindrical slice through the Galaxy to infer its radius. For example, in the inner Galaxy, all the material in a ring of radius R will lie at Galactic longitudes of less than $l_{\max} = \sin^{-1}(R/R_0)$, so one can use the extent of the emission on the sky of each W-slice to infer its radius – an approach traditionally termed the "tangent point method" [see, for example, Malhotra (1994,1995)]. At radii greater than R_0 this method is no longer applicable as the emission will be visible at all values of l. However, by assuming that the thickness of the gas layer does not vary with azimuth, one can use the observed variation in the angular thickness of the layer with Galactic longitude to estimate the radii of such W slices (Merrifield 1992).

For the remainder of this paper, we use Malhotra's (1994, 1995) tangent point analysis to estimate $W(R)$ in the inner Galaxy. For the outer Galaxy, we have combined Merrifield's (1992) data with Brand & Blitz's (1993) analysis of the distances to HII regions, from which standard candle analysis the rotation curve can be derived.

In order to convert $W(R)$ into $\Theta(R)$ using equation (1), we must adopt values for the Galactic constants, R_0 and Θ_0. Unfortunately, there are still significant uncertainties in these basic parameters. In the case of R_0, for example, the extensive review by Reid (1993) discussed measurements varying between $R_0 = 6.9 \pm 0.6$ kpc and $R_0 = 8.4 \pm 0.4$ kpc. Even more recently there have been few signs of convergence: Layden et al. (1996) used RR Lyrae stars as standard candles to derive $R_0 = 7.2 \pm 0.7$ kpc, while Feast & Whitelock (1997) used a Cepheid calibration to obtains $R_0 = 8.5 \pm 0.5$ kpc. The constraints on Θ_0 are similarly weak: a recent review by Sackett (1997) concluded that a value somewhere in the range $\Theta_0 = 210 \pm 25\,\mathrm{km\,s^{-1}}$ provided the best current estimate. It should also be borne in mind that the best estimates for R_0 and Θ_0 are not independent. Analysis of the local stellar kinematics via the Oort constants gives quite a well-constrained value for the ratio $\Theta_0/R_0 = 26.4 \pm 1.9\,\mathrm{km\,s^{-1}\,kpc^{-1}}$ (Kerr & Lynden-Bell 1986), so a lower-than-average value of R_0 is likely to be accompanied by a lower-than-average value for Θ_0. Currently, the best available measure of the local angular velocity of the Milky Way is based on VLBI proper motion measurements of SgrA*. Assuming that SgrA* is at rest with respect to the Galactic centre, Reid *etal* (1999) find: $\Omega = A - B = 27.25 \pm 2.5\,\mathrm{km\,s^{-1}\,kpc^{-1}}$, which is entirely consistent with the pre-HIPPARCOS value proposed by Kerr & Lynden-Bell.

To illustrate the effect of the adopted values of Θ_0 and R_0 on the derived rotation curve, Fig. 2 shows $\Theta(R)$ for two of the more extreme plausible sets of Galactic parameters. Clearly, the choice of values for these quantities affects such basic issues as whether the rotation curve is rising or falling in the outer Galaxy. Given the current uncertainties, it makes little sense to pick fixed values for the Galactic constants, so in the following analysis we consider models across a broad range of values, $5.5\,\mathrm{kpc} < R_0 < 9\,\mathrm{kpc}$, $165\,\mathrm{km\,s^{-1}} < \Theta_0 < 235\,\mathrm{km\,s^{-1}}$.

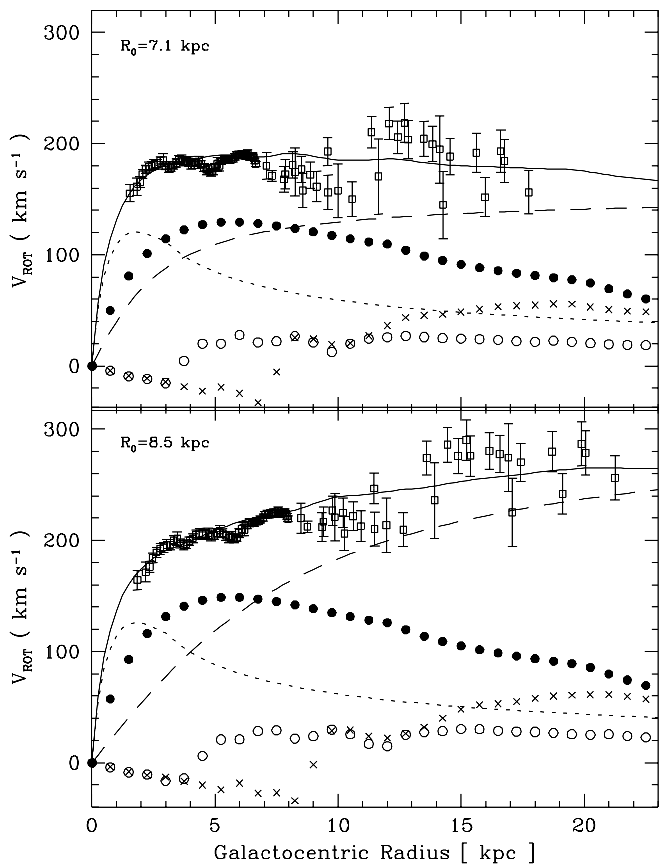

Figure 2. The rotation curve for the Milky Way for values of $R_0 = 7.1$ kpc, $\Theta_0 = 185\,\mathrm{km\,s^{-1}}$, and $R_0 = 8.5$ kpc, $\Theta_0 = 220\,\mathrm{km\,s^{-1}}$. The figure also shows one of the ways in which the rotation curve can be decomposed into the contributions from different mass components: the bulge (dotted line); the stellar disk (filled circles); the H I layer (crosses, where negative values mean that the force is directed outwards); the H_2 layer (circles); and the dark halo (dashed line). The best fit model, which is obtained by summing the individual components in quadrature, is shown as a full line.

3 MASS MODELS

In order to relate the rotation curve to the shape of the dark halo, we must break the gravitational potential responsible for the observed $\Theta(R)$ into the contributions from the different mass components. As is usually done in this decomposition (e.g. van Albada & Sancisi 1986; Kent 1987; Begeman 1989; Lake & Feinswog 1989; Broeils 1992; Olling 1995; Olling 1996c; Dehnen & Binney 1998), we adopt a model consisting of a set of basic components:

(i) *A stellar bulge.* Following Kent's (1992) analysis of the Galaxy's K-band light distribution, we model the Milky Way's bulge by a "boxy" density distribution,

$$\rho_b(R,z) \propto K_0(s/h_b), \text{ where } s^4 = R^4 + (z/q_b)^4. \quad (3)$$

This modified Bessel function produces a bulge that appears exponential in projection. The observed flattening of the K-band light yields $q_b = 0.61$, and its characteristic scalelength is $h_b = 670\,\mathrm{pc}$ (Kent 1992). The constant of proportionality depends on the bulge mass-to-light ratio, Υ_b, which we leave as a free parameter.

(ii) *A stellar disk*. The disk is modelled by a density distribution,

$$\rho_d(R,z) \propto \exp(-R/h_d)\mathrm{sech}(z/2z_e). \quad (4)$$

The first term gives the customary radially exponential disk. The appropriate value for the scalelength, h_d, is still somewhat uncertain – Kent, Dame & Fazio (1991) estimated $h_d = 3 \pm 0.5\,\mathrm{kpc}$, while Freudenreich (1998) found a value of 2.5 kpc. We therefore leave this parameter free to vary within the range $2\,\mathrm{kpc} \leq h_d \leq 3\,\mathrm{kpc}$. The z-dependence adopts van der Kruit's (1988) compromise between a sech^2 isothermal sheet and a pure exponential. For simplicity, we fix the scaleheight at $z_e = 300\,\mathrm{pc}$. However, the exact z-dependence of ρ_d has no impact on any of the following analysis. Once again, the constant of proportionality depends on the mass-to-light ratio of the disk, Υ_d, which we leave as a free parameter.

(iii) *A gas disk*. From the HI data given by Burton (1988) and Malhotra (1995) and the H_2 column densities from Bronfman et al. (1988) and Wouterloot et al. (1990), we have inferred the density of gas as a function of radius in the Galaxy. This analysis treats the gas as an axisymmetric distribution, and neglects the contribution from ionized phases of the interstellar medium, but does include a 24% contribution by mass from helium (Olive & Steigman 1995).

(iv) *A dark matter halo*. We model the dark halo as a flattened non-singular isothermal sphere, which has a density distribution

$$\rho_h(R,z) = \rho_h \frac{R_h^2}{R_h^2 + R^2 + (z/q)^2}, \quad (5)$$

where ρ_h is the central density, R_h is the halo core radius, and q is the halo flattening, which is the key parameter in this paper.

The procedure for calculating a mass model from these components is quite straightforward. For each pair of Galactic constants, R_0 and Θ_0, we vary the unknown parameters $\{\Upsilon_b, h_d, \Upsilon_d, \rho_h, R_h, q\}$ to produce the mass model that has a gravitational potential, $\Phi(R,z)$, such that

$$v(R) = \left(R \frac{\partial \Phi}{\partial R}\bigg|_{z=0} \right)^{1/2} \quad (6)$$

provides the best fit (in a minimum χ^2 sense) to the observed rotation curve, $\Theta(R)$. Examples of two such best-fit models are shown in Fig. 2.

As is well known (e.g. van Albada & Sancisi 1986; Kent 1987; Begeman 1989; Lake & Feinswog 1989; Broeils 1992; Olling 1995; Olling 1996c; Dehnen & Binney 1998), such mass decompositions are by no means unique: there is near degeneracy between the various unknown parameters, so many different combinations of the individual components can reproduce the observed rotation curve with almost equal quality of fit. We have therefore searched the entire $\{\Upsilon_b, h_d, \Upsilon_d, \rho_h, R_h, q\}$ parameter space to find the complete subset of values that produce fits in which the derived value of χ^2 exceeded the minimum value by less than unity. More details will be presented in a forthcoming paper.

4 HALO FLATTENING FROM LOCAL STELLAR KINEMATICS

Although the analysis of the previous section tells us something about the possible range of mass models for the Milky Way, it does not place any useful constraint on the shape of the dark halo: for any of the adopted values of R_0 and Θ_0, one can find acceptable mass models with highly-flattened dark halos ($q \sim 0$), round dark halos ($q \sim 1$), and even prolate dark halos ($q > 1$). We therefore need some further factor to discriminate between these models.

One such constraint is provided by stellar kinematics in the solar neighbourhood. Studies of the motions of stars in the Galactic disk near the Sun imply that the total amount of mass within 1.1 kpc of the Galactic plane is $\Sigma_{1.1} = (71 \pm 6) M_\odot\,\mathrm{pc}^{-2}$ (Kuijken & Gilmore 1991). Clearly, the value of $\Sigma_{1.1}$ provides an important clue to the shape of the Milky Way's dark halo: in general, a model with a highly-flattened dark halo will place a lot of mass near the Galactic plane leading to a high predicted value for $\Sigma_{1.1}$, while a round halo will distribute more of the dark matter further from the plane, depressing $\Sigma_{1.1}$.

The dark halo is not the only contributor to $\Sigma_{1.1}$. In particular, the stellar disk has a surface density in the solar neighbourhood, Σ_*, which may contribute a significant fraction of $\Sigma_{1.1}$. There must therefore be a fairly simple relation between the adopted value of Σ_* and the inferred halo flattening, q. Specifically, as one considers larger possible values of Σ_*, the amount of dark matter near the plane must decrease so as to preserve the observed value of $\Sigma_{1.1}$. Such a decrease can be achieved by increasing q, thus making the dark halo rounder.

This inter-relation is illustrated in Fig. 3. Here, for one of the sets of possible Galactic constants, we have considered all the mass models that produce an acceptable fit to the rotation curve. For each acceptable model, we have extracted the value of the halo flattening q and the mass of the stellar disk in the solar neighbourhood, Σ_*. For the reasons described above, these quantities are tightly correlated, and Fig. 3 shows the linear regression between the two.

Clearly, we have not yet derived a unique value for the halo flattening: by selecting models with different values of Σ_*, we can still tune q to essentially any value we want. However, Σ_* is not an entirely free parameter. From star-count analysis, it is possible to perform a stellar mass census in the solar neighbourhood, and thus determine the local stellar column density. Until relatively recently, this analysis has been subject to significant uncertainties, with estimates as high as $\Sigma_* = 145 M_\odot\,\mathrm{pc}^{-2}$ (Bahcall 1984). However, there is now reasonable agreement between the various analyses, with more recent published values of $35 \pm 5 M_\odot\,\mathrm{pc}^{-2}$ (Kuijken & Gilmore 1989) and $26 \pm 4 M_\odot\,\mathrm{pc}^{-2}$ (Gould, Bahcall & Flynn 1997). If we adopt Kuijken & Gilmore's slightly more conservative error bounds on Σ_*, the shaded regions in Fig. 3 no longer represent acceptable models as they predict the wrong local disk mass density, so we end up with a

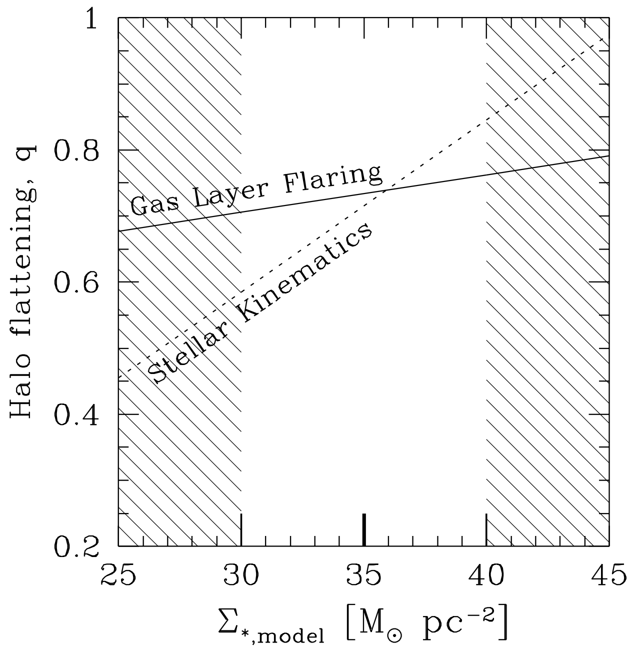

Figure 3. The flattening of the model Galactic halo, q, as a function of the adopted model's column of stellar disk mass in the Solar neighbourhood, Σ_*. We show the best fits to the stellar kinematic constraints (dotted line) and the flaring of the HI layer (full line). The shaded region shows values of Σ_* that lie more than 1-σ from the observed value. This particular set of calculations has been made assuming $R_0 = 7.1\,\mathrm{kpc}$ and $\Theta_0 = 185\,\mathrm{km\,s^{-1}}$.

moderately well-constrained estimate for the halo flattening of $q = 0.7 \pm 0.1$.

Note, though, that although this analysis returns a good estimate for q, Fig. 3 only shows the value obtained for a particular set of Galactic constants. As discussed above, changing the adopted values for R_0 and Θ_0 alters the range of acceptable mass models, which, in turn, will alter the derived correlation between Σ_* and q. The uncertainties in the Galactic constants are still sufficiently large that the absolute constraints on q remain weak. Nevertheless, it is to be hoped that the measurements of R_0 and Θ_0 will continue to improve over time, leading to a unique determination of q by this method. Further, as we shall see below, it may be possible to attack the problem from the other direction by using other estimates of q to help determine the values of the Galactic constants.

5 HALO FLATTENING FROM GAS LAYER FLARING

We now turn to the technique developed by Olling (1995) for measuring the shape of a dark halo from the observed thickness of a galaxy's gas layer. In essence the approach is similar to the stellar-kinematic method described above: the over-all mass distribution of the Milky Way is inferred from its rotation curve, while the degree to which this mass distribution is flattened is derived using the properties of a tracer population close to the Galactic plane. In this case, the tracer is provided by the HI emission from the Galactic gas layer. The thickness of the Milky Way's gas layer is dictated by the hydrostatic balance between the pull of gravity toward the Galactic plane and the pressure forces acting on the gas. As the density of material in the Galaxy decreases with radius, the gravitational force toward the plane becomes weaker, so the equilibrium thickness of the layer becomes larger, giving the gas distribution a characteristic "flared" appearance. The exact form of this flaring depends on the amount of mass close to the plane of the Galaxy. Thus, by comparing the observed flaring to the predictions of the hydrostatic equilibrium arrangement of gas in the mass models developed in Section 3, we can see what degree of halo flattening is consistent with the observations.

5.1 The observed flaring of the gas layer

Before we can apply this technique, we need to summarize the observational data available on the flaring of the Galactic HI layer. Merrifield (1992) calculated the thickness of the gas layer across a wide range of Galactic azimuths in his analysis of the outer Galaxy rotation curve. As a check on the validity of that analysis, we have also drawn on the work of Diplas & Savage (1991) and Wouterloot et al. (1992), which derived the gas layer thicknesses across a more limited range of azimuths. For completeness, we have also included the data for the inner Galaxy as derived by Malhotra (1995). The resulting values for the full-width at half maximum (FWHM) of the density of gas perpendicular to the plane are given in the upper panel in Fig. 4. Note that, once again, the results depend on the adopted values of the Galactic constants – since the radii in the Galaxy of the various gas elements were derived from their line-of-sight velocities via equations (1) and (2), the values of R in Fig. 4 depend on R_0 and Θ_0[‡].

It would appear from this figure that there are some discrepancies between the various measurements in the outer Galaxy. After some investigation, we established that these differences can be attributed to the effects of the beam sizes of the radio telescopes with which the observations were made. Such resolution effects will mean that the FWHM of the gas will tend to be overestimated. In the lower panel, we show what happens when the appropriate beam correction is made to the data from Diplas & Savage (1991) and Wouterloot et al. (1992). No similar correction is required for the Merrifield (1992) analysis, as in that work the derived value of the FWHM was dominated by gas towards the Galactic anti-centre, which lies at relatively small distances from the Sun, and so the beam correction is small. Clearly, this correction brings the various data sets into much closer agreement. We therefore adopt the mean curve shown in this panel for the following analysis; the error bars shown rep-

‡ Merrifield's method to determine the thickness of the gas layer also exposes some of the shortcomings of more traditional methods. If the wrong values for R_0, Θ_0 and $\Theta(R)$ are chosen, the inferred thickness of the gas layer (at a given R) will show a systematic variation with Galactocentric azimuth. It is possible to correct published data for this effect, but only if the assumed rotation curve, Galactic constants, as well as the thickness of the gas layer as a function of azimuth are specified.

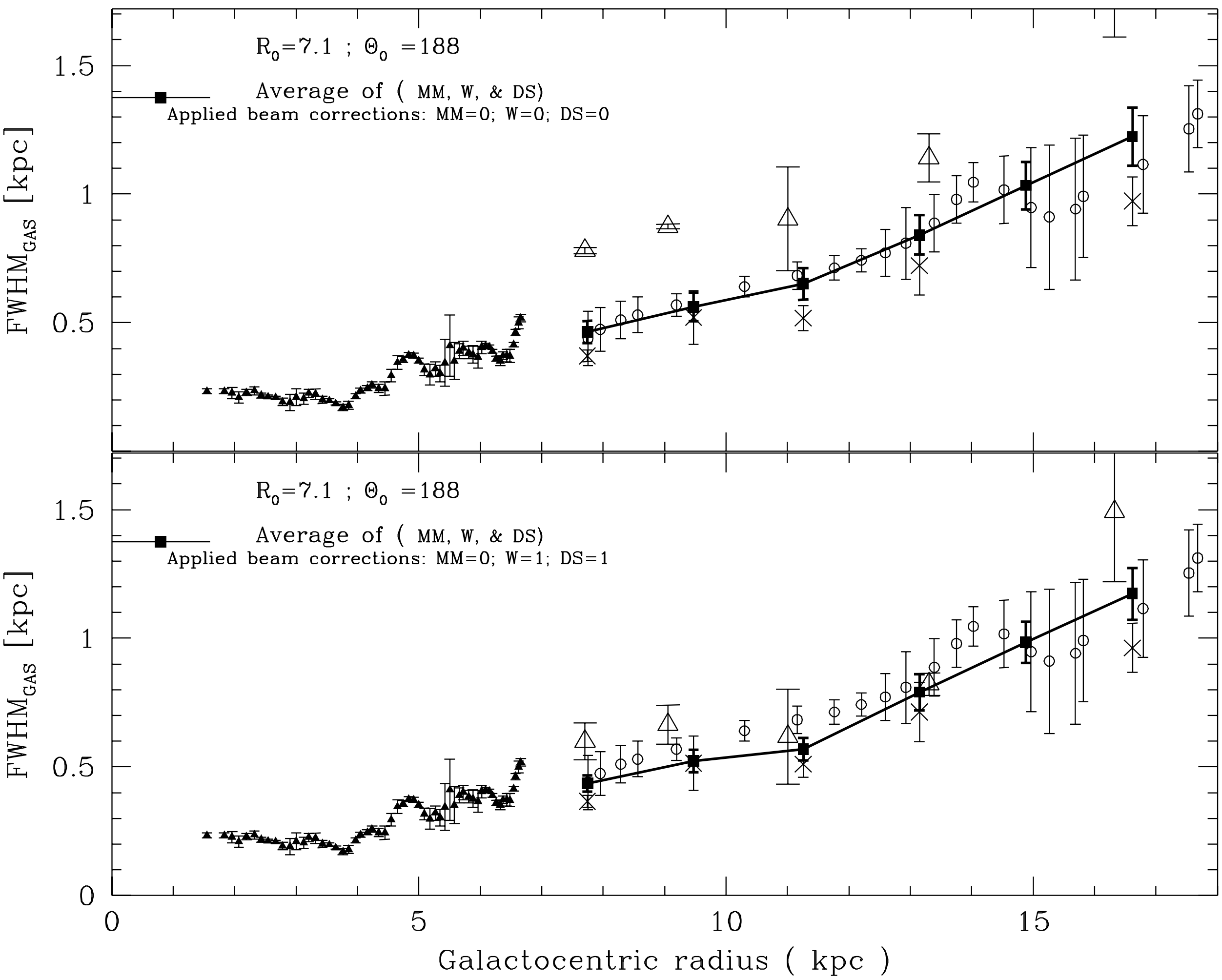

Figure 4. The thickness of the HI layer of the Milky Way. The widths in the inner Galaxy were taken from Malhotra (1995). For the outer Galaxy, we plot the widths from Diplas & Savage (1991; open triangles), Wouterloot et al. (1992; crosses), Merrifield (1992; open circles), and the average (thick full line & filled squares). The top panel represents the "raw" measurements, in bottom panel we present the beam-size corrected widths.

resent the standard error obtained on averaging the various determinations.

5.2 Sources of pressure support

In order to compare the observed gas layer flaring to the predictions for a gas layer in hydrostatic equilibrium, we must address the source of the pressure term in the hydrostatic equilibrium equation. The most obvious candidate for supporting the HI layer comes from its turbulent motions. In the inner Galaxy, the HI gas is observed to have a velocity dispersion of $\sigma_g = 9.2\,\mathrm{km\,s^{-1}}$ independent of radius (Malhotra 1995), and we assume that this value characterizes the turbulent motions of the gas throughout the Galaxy, providing a kinetic pressure term.

Potentially, there may be other forces helping to support the Galactic HI layer: non-thermal pressure gradients associated with magnetic fields and cosmic rays may also provide a net force to resist the pull of gravity on the Galactic HI. However, the analysis we are doing depends most on the properties of the HI layer at large radii in the Milky Way, where star formation is almost non-existent, so energy input into cosmic rays and magnetic fields from stellar processes is likely to be unimportant.

Our concentration on the properties of gas at large radii also eliminates another potential complexity. In the inner Galaxy, the interstellar medium comprises a complicated multi-phase mixture of molecular, atomic and ionized material. A full treatment of the hydrostatic equilibrium of such a medium is complicated, as gas can transform from one component to another, so all components would have to be considered when calculating hydrostatic equilibrium. For the purpose of this paper, it is fortunate that at the low pressures characteristic of the outer Galaxy it is not possible to maintain both the cold molecular phase and the warm atomic phase (Maloney 1993; Wolfire et al. 1995). Braun and collaborators (1992, 1997, 1998) has shown that the cold phase disappears when the B-band surface brightness of a galaxy falls below the 25th magnitude per square arcsecond level, which occurs at $\sim 1.5R_0$ in the Milky Way (Binney &

Merrifield 1998). Further, the ionized fraction of the ISM is expected to decrease with distance as it is closely associated with sites of star formation (Ferguson et al. 1996; Wang, Heckman & Lehneert 1997). Ultimately, the ionizing effects of the extragalactic background radiation field become significant, but only when the HI column density falls below about $1 M_{\odot}\,\mathrm{pc}^{-2}$ (Maloney 1993; Dove & Shull 19944; Olling 1996c), which lies well beyond the radii we are considering here.

For the current analysis, it therefore seems reasonable to treat the Milky Way's gas layer as a single isothermal component supported purely by its turbulent motions. Moreover, this assumption has been made in the previous implementations of the gas flaring method (Olling 1996b; Becquaert, Combes & Viallefond 1997). A principal objective of this paper is to test the validity of those analyses by comparing results obtained by the flaring technique to those obtained by other methods. It is therefore important that we make the same assumption of a single isothermal component in the present study.

5.3 Fitting to model gas layer flaring

We are now in a position to compare observation and theory. The technique for calculating the gas layer thickness in different mass models has been described in detail by Olling (1995). In brief, for each model, at each radius R, one integrates over the full model density distribution to obtain the vertical force law, $\partial\Phi/\partial z$. One integrates the hydrostatic equilibrium equation,

$$\frac{\partial \Phi}{\partial z} = -\frac{1}{\rho_g}\frac{\partial \rho_g \sigma_g^2}{\partial z}, \tag{7}$$

to obtain the gas density distribution, $\nu_g(R, z)$. The FWHM of this model gas distribution can then be compared directly with the observations.

The results of such calculations are illustrated by the examples shown in Fig. 5. The basic trends in this analysis is clearly demonstrated by these examples. The decrease in total density with radius leads to a dramatic flaring in the model-predicted gas layer thickness, which is also seen in the observations. For a flatter model dark halo, the mass is more concentrated toward the plane of the Galaxy, squeezing the HI layer into a thinner distribution.

Once again, the results depend quite sensitively on the choice of Galactic constants, since these values affect both the gas distribution as inferred from observations and the acceptable mass models as inferred from the rotation curve. As is apparent from Fig. 5, none of the $R_0 = 8.5\,\mathrm{kpc}$ models fit the observations. In fact, to match the observed layer width one would require a substantially prolate dark matter halo with $q \sim 1.5$, which none of the current dark matter scenarios predict. For $R_0 = 7.1\,\mathrm{kpc}$, on the other hand, a very good fit is obtained for models with a halo flatness of $q \sim 0.7$. Such models even reproduce the observed inflection in the variation of the gas layer width with radius at $R \sim 10\,\mathrm{kpc}$.

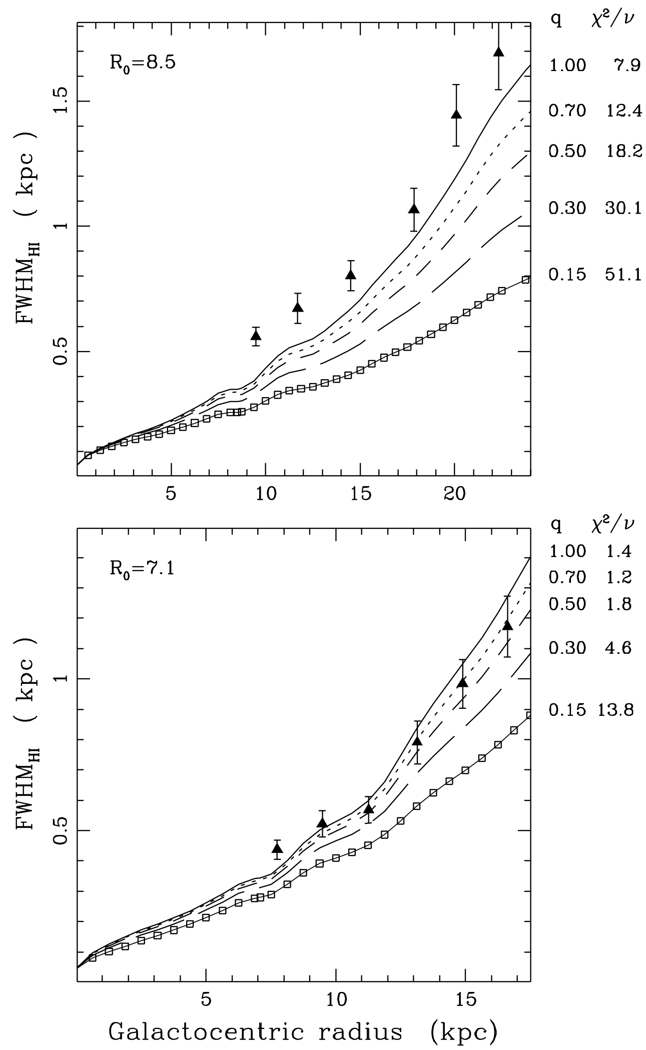

Figure 5. The observed flaring of the Galaxy's gas layer (triangles) compared with the flaring predicted for a number of mass models that reproduce the observed rotation curve and value of Σ_*. The models in the top panel have been calculated assuming $R_0 = 8.5\,\mathrm{kpc}$ and a disk mass-to-light ratio $\Upsilon_{\mathrm{d,K-band}} = 0.60$; the bottom panel shows models with $R_0 = 7.1\,\mathrm{kpc}$ and $\Upsilon_{\mathrm{d,K-band}} = 0.41$. The models shown here have a disk scale-length of $h_d = 2.5\,\mathrm{kpc}$. The halo flattening of the model and the reduced χ^2 value of the fit is shown for each case.

For each plausible set of Galactic constants, we can carry out a similar analysis to that in Section 4 to see what range of values of q are consistent with the observed gas layer flaring. Because this technique relies on data from large radii in the Galaxy, where the dark matter halo is the dominant source of mass, the flaring predicted by the models depends very little on the properties of the disk and bulge. Unlike the stellar kinematic analysis, therefore, one cannot trade off the mass in the disk against the mass near the plane from a more-flattened dark halo. This difference is illustrated in Fig. 3, which shows the way that the value of q inferred from the gas layer flaring depends on the properties of the stellar disk (as parameterized by the model's column density of stars in the Solar neighbourhood). As for the stellar-kinematic analysis, there is a well-defined correlation between q and Σ_*, but, for the reasons described above, the trend for the current method is very much weaker, and, within the observationally-allowed range for Σ_*, q is tightly constrained to 0.73 ± 0.03.

Although this constraint is remarkably good, it should be borne in mind that it is still dependent on the adopted values for the Galactic constants. As we have seen above, larger values for R_0 lead to rounder, or even prolate estimates for halo shape, so we will not obtain an unequivocal measure for q from this method until the Galactic constants are measured more accurately

6 COMBINING THE TECHNIQUES

The different slopes of the two relations in Fig. 3 raises an interesting possibility. Clearly, for a consistent picture, one must use a single mass model to reproduce both the stellar-kinematic constraint on the mass in the solar neighborhood and the observed flaring of the gas layer. Thus, although there are whole linear loci in this figure of models with different values of q and Σ_* that satisfy each of these constraints individually, there is only the single point of intersection between these two lines where the model fits both the stellar-kinematic constraint and the observed flaring of the gas layer. Hence, for given values of R_0 and Θ_0, one predicts unique values for q and Σ_*.

We have therefore repeated the analysis summarized in Fig. 3 spanning the full range of plausible values for R_0 and Θ_0, and calculated the mutually-consistent estimates for Σ_* and q for each case. In order to reduce the computational complexity of this large set of calculations to manageable proportions, we made use of Olling's (1995 Appendix D) fitting formulae, which showed that, if self-gravity is negligible, one can approximate the model-predicted thickness of the gas layer by the relation

$$\mathrm{FWHM}(R) \approx \sqrt{\frac{13.5q}{1.4+q}\frac{\sigma_g}{v_{h,\infty}}}\sqrt{R_h^2+R^2}, \tag{8}$$

where $v_{h,\infty}$ is the circular rotation speed of the dark halo component at large radii. We compare the values found from a similar formula which includes the effects of the gaseous self-gravity[§] to sample results obtained by the full integration process described above. We found that the approximation formulae based on equation (8) match the detailed integration for $R > 1.75R_0$. We therefore only used the data from beyond this radius in the following analysis.

The values obtained for q and Σ_* for each possible pair of Galactic constants are presented in Fig. 6. Thus, for example, for values of $R_0 = 7.1$ kpc and $\Theta_0 = 185\,\mathrm{km\,s^{-1}}$, one finds $\Sigma_* = 35 M_\odot\,\mathrm{pc^{-2}}$ and $q = 0.7$, corresponding to the intercept that we previously calculated in Fig. 3.

Figure 6 places some interesting limits on the properties of the Milky Way. For example, if we maintain our prejudice that the halo should be oblate ($q < 1$), then, unless we adopt a particularly extreme value for R_0, we find that Θ_0 must be less than $\sim 190\,\mathrm{km\,s^{-1}}$. If we also adopt Kuijken & Gilmore's (1989) measurement of $\Sigma_* = 35 \pm 5 M_\odot\,\mathrm{pc^{-2}}$, we find that only models within the heavily-shaded region of Fig. 6 are acceptable, placing an upper limit on R_0 of ~ 7.6 kpc. Conversely, if one forces the Galactic constants to the IAU standard values of $R_0 = 8.5$ kpc and $\Theta_0 = 220\,\mathrm{km\,s^{-1}}$ (Kerr & Lynden-Bell 1987), one finds barely-credible values of $\Sigma_* \sim 60 M_\odot\,\mathrm{pc^{-2}}$ and $q \sim 1.5$.

7 CONCLUSIONS

The prime objective of this paper has been to check the validity of techniques for measuring halo flattening by asking whether two different techniques return consistent values when applied to the Milky Way. As we have seen in the last section, the answer is a qualified "yes." The qualification is that consistency with the measured stellar column density requires values of the Galactic constants that differ from those conventionally adopted. However, as was discussed in Section 2, the true values of these constants remain elusive, with estimates spanning the ranges $7\,\mathrm{kpc} < R_0 < 8.5\,\mathrm{kpc}$ and $185\,\mathrm{km\,s^{-1}} < \Theta_0 < 235\,\mathrm{km\,s^{-1}}$. With such gross uncertainties, it quite straightforward to pick values that produce an entirely self-consistent picture. To underline this point, we have included on Fig. 6 the results of Olling & Merrifield's (1997) estimates for R_0 and Θ_0 derived from an analysis of the Oort constants. If that analysis is valid, then we have a consistent model for the Milky Way in which the dark halo has a flattening of $q \sim 0.8$.

Ultimately, this analysis will allow us to come to one of three conclusions:

(i) If future studies confirm low values for R_0 and Θ_0 similar to those derived by Olling & Merrifield (1997), then the consistency of the two analyses for calculating q imply that the gas layer flaring technique is valid, adding confidence to the previous determinations by this method.

(ii) Conversely, if we learn in future that R_0 and Θ_0 are closer to the more conventional larger values, then the implied values of Σ_* are so far from the observed estimates that one has to suspect that at least one of the techniques for measuring q is compromised. In this case, one would have to look more closely at some of the assumptions that went into the analysis. For example, perhaps the non-thermal pressure forces from cosmic rays and magnetic fields have a role to play even at large radii in galactic disks. Alternatively, perhaps the HI layer is not close enough to equilibrium for the hydrostatic analysis to be valid.

(iii) Our assumption of azimuthal symmetry may be invalid. This could mean that the determination of the thickness and column density of the gas presented here is not correct, and that the locally determined values of $\Sigma_{1.1}$ and Σ_* may not be representative for the Galactocentric radius of the Sun.

Assuming for the moment that the analysis is valid, we have another datum to add to Fig. 1. Since the two previous flaring analyses returned systematically rather small values of $q \sim 0.3$, it is reassuring that the Milky Way seems to indicate a larger value of ~ 0.8 – it appears that the low values are simply a coincidence arising from the very small number statistics. This larger value is inconsistent with the very flat halos that are predicted by models in which the dark matter consists of either decaying neutrinos (Sciama 1990) or cold molecular hydrogen (Pfenniger, Combes & Martinet 1994).

[§] If the self-gravity of the gas is neglected, equation (8) would under-predict the gas layer widths by up to 50% (Olling 1995, 1996c.

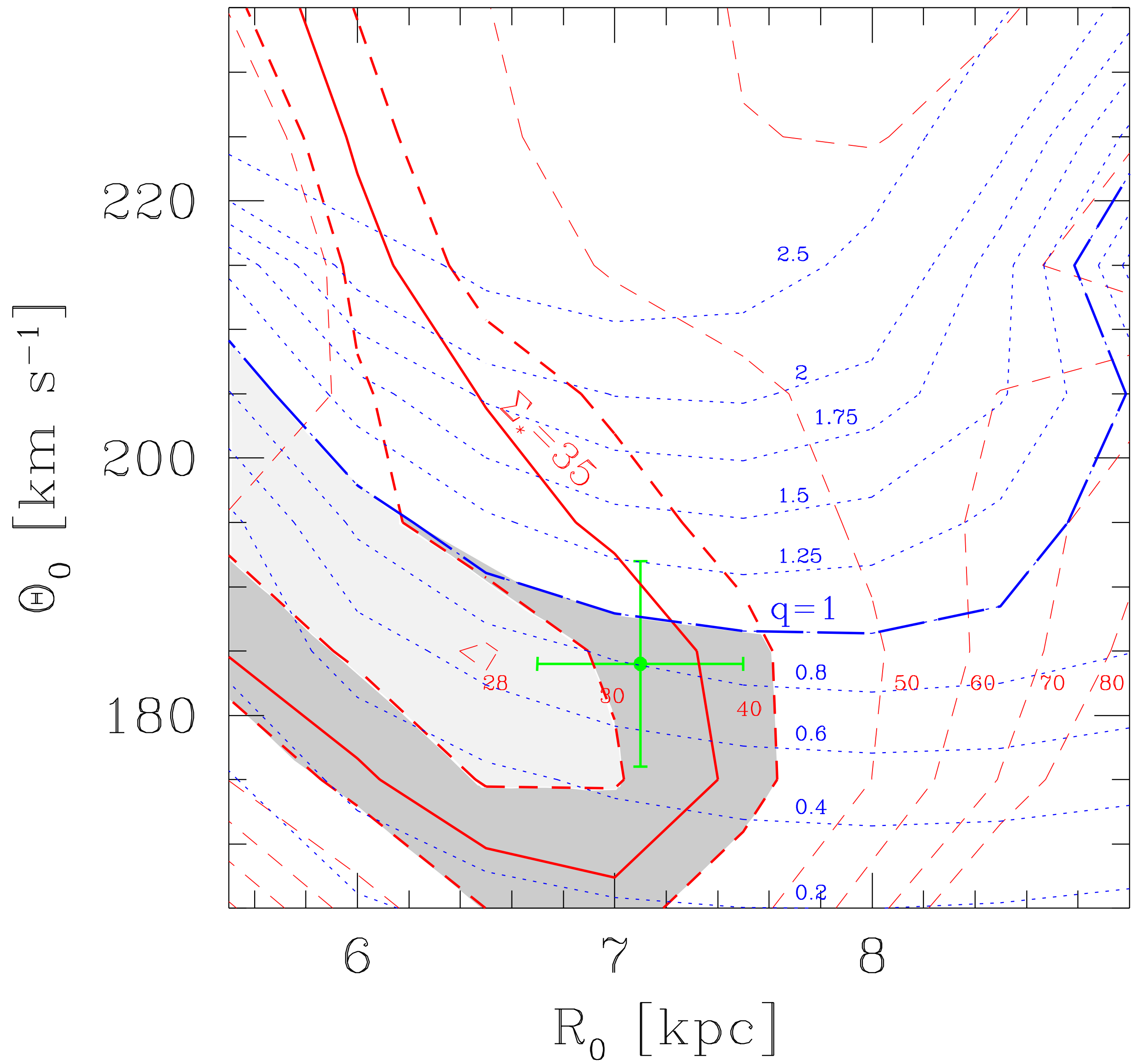

Figure 6. Contours of the stellar column density in the Solar neighbourhood (Σ_*; long dashed lines) and halo flattening (q; dotted lines) as a function of the adopted values for the Galactic constants, R_0 and Θ_0. The heavy full line and the heavy dashed line corresponds to Kuijken & Gilmore's (1989) determination of Σ_*, and the $\pm 1-\sigma$ values. The heavily-shaded region corresponds to parts of parameter space consistent with these values of Σ_* that produce an oblate halo. The lightly-shaded area gives the corresponding region if we adopt Gould, Bahcall and Flynn's (1997) values for Σ_*. The cross shows the determination of the Galactic constants based on an analysis of the Oort constants (Olling & Merrifield 1998).

With the addition of the Milky Way to the data presented in Fig. 1, the only technique that stands out as giving systematically different values for q is the bending mode analysis of warped gas layers. In this regard, it is notable that simulations cast some doubt on the validity of such analyses, since it appears that dynamical friction between a flexing disk and a surrounding dark halo tends to suppress the persistent bending modes that the method assumes are responsible for warps (e.g. Dubinski & Kuijken 1995, Nelson & Tremaine 1995, Binney, Jiang & Dutta 1998). The number of measurements is still rather small, but it is at least interesting that if one neglects the warped gas layer results, the remaining data appear entirely consistent with the dotted line in Fig. 1, which shows Dubinski's (1994) prediction for the distribution of halo shapes that will be produced in a cold dark matter cosmology.

ACKNOWLEDGMENTS

We would like to thank Andy Newsam, Irini Sakelliou, Konrad Kuijken, Marc Kamionkowski and Jacqueline van Gorkom for useful discussions. We are also very grateful to the referee, James Binney, for his major contribution to the clarity of this paper.

REFERENCES

Arnaboldi M., Capaccioli M., Cappellaro E., Held E.V., Sparke L.S., 1993, A&A, 267, 21
Bahcall J.N., 1984, ApJ, 276, 169
Becquaert J.F., Combes F., Viallefond F. 1997, A&A, 325, 41
Begeman K., 1989, A&A, 223, 47
Binney J.J., Merrifield M.R., 1998, Galactic Astronomy, Princeton University Press
Binney J.J., Jiang I.G., Dutta S., 1998, MNRAS, 297, 1237
Bosma A., 1981, AJ, 86, 1825
Brand J. & Blitz L., 1993, A&A, 275, 67
Braun R., 1998, in Franco J., Carraminana A., eds, Interstellar Turbulence, Proceedings of the 2nd Guillermo Haro Conference, Cambridge University Press.
Braun R., 1997, ApJ, 484, 637
Braun R., Walterbos R.A.M., 1992, ApJ, 386, 120
Bronfman L., Cohen R.S., Alvarez H., May J. & Thaddeus P., 1988, ApJ, 324, 248
Broeils A., 1992, Ph. D. Thesis, University of Groningen
Buote D.A., Canizares C.R., 1996, ApJ, 468, 184
Buote D.A., Canizares C.R., 1998, MNRAS, 298, 811
Dehnen W., Binney J., 1998, MNRAS, 294, 429
Diplas A. & Savage D.S., 1991, ApJ, 377, 126
Dove J.D., Shull J.M., 1994, ApJ, 423, 196
Dubinski J., 1994, ApJ, 431, 617
Dubinski J., Kuijken K., 1995, ApJ, 442, 492
Feast M., Whitelock P., 1997, MNRAS, 291, 683
Ferguson A.M.N., Wyse R.F.G., Gallagher J.S., Hunter D.A., 1996, AJ, 111, 2265
Gould A., Bahcall J.N., Flynn C. 1997, ApJ, (GBF97)
Hofner P. & Sparke L., 1994, ApJ, 428, 466
Katz N., Gunn J.E., 1991, ApJ, 377, 365
Kent S.M., 1987, AJ, 93, 816
Kent S.M., Dame T.M. & Fazio G., 1991, ApJ, 378, 131
Kerr F.J., Lynden-Bell D., 1986, MNRAS, 221, 1023
Kuijken K. & Gilmore G., 1991, ApJl, 367, L9 (KG91)
Kuijken K. & Gilmore G., 1989b, MNRAS, 239, 605
Lake G., Feinswog L., 1989, AJ, 98, 166
Layden A.C., Hanson R.B., Hawley S.L., Klemola A.R., Hanley C.J., 1996, AJ, 112, 2110
Malhotra S., 1995, ApJ, 448, 138
Malhotra S., 1994, ApJ, 443, 687
Maloney P., 1993, ApJ, 414, 41
Merrifield M.R., 1992, AJ, 103, 1552
Nelson R.W., Tremaine S., 1995, MNRAS, 275, 897
Olling R.P., Merrifield M.R., 1998, MNRAS, 295, 737
Olling R.P., 1996b, AJ, 112, 481-490
Olling R.P., 1996c, AJ, 112, 457-480
Olling R.P., 1995, AJ, 110, 591
Peebles P.J.E., 1993, "Principals of Physical Cosmology", Princeton University Press
Pfenniger D., Combes F., & Martinet L., 1994, A&A, 285, 79
Reid M.J., Readhead A.C.S., Vermeulen R.C., Treuhaft R.N., 1999, astro-ph/9905075
Reid M.J., 1993, ARA&A, 31, 345
Rubin V.C., Ford W.K., Thonnard N., 1980, ApJ, 238, 471
Sackett P.D., 1997, ApJ, 483, 103
Sackett P.D. & Pogge R.W. in *Dark Matter*, edited by S.S. Holt, C.L. Bennet (AIP conference proceedings 336), 1995, p. 141
Sackett P.D., Rix H.W., Jarvis B.J. & Freeman K.C., 1994, ApJ, 436, 629
Sciama D., 1990, MNRAS, 244, 1
Steiman-Cameron T.Y., Kormendy J. & Durisen R.H., 1992, AJ, 104, 1339
Udry S. & Martinet L., 1994, A&A, 281, 314
Albada T.S. van & Sancisi R., 1986, Phil. Trans. R. Soc. Lond. A., 320, 447
Wang J., Heckman T.M., Lehnert M.D., 1997, ApJ, 491, 114
Warren M.S., Quinn P.J., Salmon J.K., Zurek W.H., 1992, ApJ, 399, 405
Wolfire M.G., Hollenbach D., McKee C.F., Tielens A.G.G.M., Bakes E.L.O., 1995, ApJ, 443, 152
Wouterloot J.G.A., Brand J., Burton W.B. & Kwee K.K., 1990, A&A, 230, 21